Table 1 Coefficients and exponents of power functions for $St_r/St_{r,90}$, $\bar{f}/\bar{f}_{90}$, and $[(St_r/St_{r,90})/(\bar{f}/\bar{f}_{90})^{1/3}]$

	$St_r/St_{r,90}$		$\bar{f}/\bar{f}_{90}$		$(St_r/St_{r,90})/(\bar{f}/\bar{f}_{90})^{1/3}$	
Case/Angle	a	b	a	b	a	b
[3]/90 deg	1.53	−0.0035	0.74	0.0784	1.69	−0.0297
[4]/45 deg	2.84	−0.0716	1.94	−0.0640	2.27	−0.0503
[5]/60 deg	2.33	−0.0485	1.04	0.0286	2.30	−0.0580
[6]/±45 deg	2.63	−0.0658	1.87	−0.0257	2.14	−0.0573
[7]/±60 deg	3.16	−0.0748	1.68	0.0123	2.66	−0.0789
[8]/±120 deg	1.22	0.0129	0.47	0.1148	1.57	−0.0254
[9]/±135 deg	2.27	−0.0521	0.99	0.0265	2.28	−0.0609

squares straight lines through experimental data of Lau et al.[3]) are included for comparison.

All arrays of discrete ribs in this study enhance more heat transfer from the ribbed walls than 90 deg full ribs. Discrete ribs with α = 60 deg, ±60 deg, and ±120 deg (Cases 5, 7, and 8) generally cause higher heat transfer from the ribbed walls than discrete ribs with α = 45 deg, ±45 deg, and ±135 deg (Cases 4, 6, and 9). Among the angled discrete ribs, ±60 deg discrete ribs have the highest values of St_r. Discrete ribs with α = 90 deg (Case 3) have the highest values of St_r at large Re_D. Angled discrete ribs enhance more heat transfer from the ribbed walls than the corresponding 60 deg and 45 deg full ribs (Cases 1 and 2). The interactions between separated flows from the various edges of the discrete ribs, including those at the ends, and secondary flows are believed to cause better mixing in the flow and the generally higher heat transfer in the discrete rib cases than in the corresponding full rib cases.

Replacing the full ribs with discrete ribs in Cases 6 and 7 (α = ±45 deg and ±60 deg) also increases the heat transfer from the smooth walls. The smooth-wall Stanton numbers for other angled discrete ribs, however, are generally lower than those for full ribs with α = 60 deg and 45 deg, respectively. Discrete ribs with α = 90 deg have by far the lowest values of St_s.

Discrete ribs with α = 45 deg and 60 deg (Cases 4 and 5) cause about the same pressure drop as the 45 deg and 60 deg full ribs, respectively. Other discrete ribs cause higher pressure drop than corresponding full ribs. Among the discrete rib cases in this study, 45 deg discrete ribs (Case 4) have the lowest friction factor and ±60 deg discrete ribs (Case 7) the highest.

Figure 3 compares the thermal performances of the discrete ribs with those of the angled full ribs. The ratios $[(St_r/St_{r,90})/(\bar{f}/\bar{f}_{90})^{1/3}]$ and $[(\overline{St}/\overline{St}_{90})/(\bar{f}/\bar{f}_{90})^{1/3}]$ for all cases are plotted versus Re_D. Among the cases studied, discrete ribs with α = 45 deg (Case 4) have the best thermal performance. Their performance, however, is lower than those of parallel staggered 3 × 2 discrete-rib arrays with α = 45 deg and 60 deg (Lau et al.[3]).

Discrete ribs with α = 90 deg enhance more heat transfer from the ribbed walls (up to 50%) than 90 deg ribs but cause much higher pressure drops (up to 75%). On a per unit pumping power basis, 90 deg discrete ribs have high ribbed wall heat transfer but low overall heat transfer.

The coefficients and exponents of power functions of the Reynolds number, $a(Re_D)^b$, for $St_r/St_{r,90}$, $\bar{f}/\bar{f}_{90}$, and $[(St_r/St_{r,90})/(\bar{f}/\bar{f}_{90})^{1/3}]$ are given in Table 1. The power functions are determined by curve fitting least-squares straight lines through the experimental data.

Concluding Remarks

Discrete ribs with α = ±60 deg and 90 deg cause very high heat transfer from the ribbed walls. Discrete ribs with α = 45 deg (Case 4) have the best thermal performance. Replacing angled full ribs with these discrete ribs in cooling channels in turbine airfoils improves the thermal performance of the channels.

Acknowledgments

This research was supported by the National Science Foundation (Grant CTS-8910860).

References

[1]Burggraf, F., "Experimental Heat Transfer and Pressure Drop with Two-Dimensional Turbulence Promoter Applied to Two Opposite Walls of a Square Tube," *Augmentation of Convective Heat and Mass Transfer*, edited by A. E. Bergles and R. L. Webb, American Society of Mechanical Engineers, New York, 1970, pp. 70–79.

[2]Han, J. C., Park, J. S., and Lei, C. K., "Heat Transfer Enhancement in Channels with Turbulence Promoters," *ASME Journal of Engineering for Gas Turbines and Power*, Vol. 107, July 1985, pp. 629–635.

[3]Lau, S. C., McMillin, R. D., and Han, J. C., "Heat Transfer Characteristics of Turbulent Flow in a Square Channel with Angled Discrete Ribs," ASME Paper 90-GT-254, 1990, and *ASME Journal of Turbomachinery*, Vol. 113, July 1991, pp. 367–374.

[4]Chyu, M. K., and Natarajan, V., "Local Heat Transfer on a Flat Surface Roughened with Broken Ribs," presented at the 1989 ASME Winter Annual Meeting, San Francisco, CA, ASME HTD-Vol. 120, 1989, pp. 25–31.

Practical Method for Calculating Radiation Incident upon a Panel in Orbit

Masao Furukawa*
National Space Development Agency, Tsukuba, Ibaragi 305, Japan

Introduction

DETERMINATION of external radiation incident upon flat plates or area elements is indispensable for thermal design practice of a satellite for which temperatures will passively be controlled. In determining radiant transfer from the sun or the earth to a specified surface, one needs a precise knowledge of angle factors showing the rates of radiation directly intercepted by the surface. Such view factors was first considered by Katz[1] and then by Hrycak,[2] and some of them were calculated by Ballinger et al.[3] Cunningham[4,5] presented analytical expressions of earth-reflected solar radiation input to spherical satellites. Also given by Cunningham[6–8] are expressions for calculating thermal radiation from the earth

Received May 18, 1990; revision received Aug. 7, 1990; accepted for publication Aug. 16, 1990.

*Senior Engineer, System Engineering Division, Tsukuba Space Center, 2-1-1, Sengen.

to a flat plate spinning or not and those for evaluating earth-reflected solar radiation incident upon a spinning one. Then, Powers[9] introduced vector representations which permit computations of total thermal radiation to a flat plate rotating about an arbitrary axis. For readily making an estimate of the view factor between the earth and a cylinder or flat plate, Bannister[10] derived polynomial equations expressed in terms of altitude and attitude angle. Watts[11] then proposed to place the defining coordinate system in the satellite rather than in the earth for an easier evaluation of radiant heating. Computer programs were also developed by Skladany and Rochkind,[12] Doenecke,[13] and Finch et al.[14] with the object of finding net heat input to an earth satellite with a more complex geometry or to a moon orbiter.

The method for calculating external radiation input was, thus, well established in 1960s. After that, no special attention has, therefore, been paid to this subject. However, with a recent progress in projects on various types of spacecraft, technical concern is again directed to net thermal energy incident upon a radiator panel which will usually be an oriented flat plate. From an angle of calculations for radiator panel sizing, the expressions or equations obtained before[2-11] seem rather sophisticated except those of Bannister[10] or Watts.[11] Although the method of Bannister[10] has widely been employed until now, one has no more geometry factors than those shown in the tables.[10] Then, even if one employs the method of Watts,[11] there still remains integral expressions which are quite impossible to give analytical results except the cases of spherical or hemispherical satellites. In addition, a simple approximate relation suggested by them[10,11] can be too rough to evaluate albedo geometry factors. The programs mentioned above[12-14] and also standard computer codes as NEVADA[15] or TRASYS will make possible a more precise evaluation of such factors.[16] However, the use of them[12-16] usually involves complications in data arrangement and a considerable amount of computation time. For that reason, this paper presents a practical method which facilitates numerical computations of radiation input to a radiator panel.

General Expressions

Earth- and albedo-radiation incident upon a flat plate in orbit, Φ_e and Φ_a, can generally be written as

$$\Phi_e = I_e F_e \tag{1a}$$

$$\Phi_a = I_a F_a \tag{1b}$$

where I_e is the earth-emitted radiant flux, I_a the earth-reflected solar flux, F_e the earth view factor, and F_a the albedo view factor. As seen in the literature,[2,3,13,14] the fluxes are expressed as

$$I_e = I_s(1 - \rho_a)/4 \tag{2a}$$

$$I_a = I_s \rho_a \tag{2b}$$

where I_s is the solar constant, and ρ_a the albedo factor (ratio of earth-reflected to earth-received solar energy). Equation (2a) can readily be derived from an equation describing thermal balance of the earth. Considering seasonal variations of the solar irradiance, one has

$$I_s = \bar{I}_s(1 + e_s \cos\nu_s)^2 \tag{3}$$

where $\bar{I}_s$ is the mean solar constant, 1353W/m^2, e_s the eccentricity of the earth's orbit about the sun, and ν_s the true anomaly of the sun on the ecliptic. Then, according to Skylab data,[17] the albedo considerably depends on orbit inclination. The data is well correlated with the inclination i and may be reduced to an empirical expression

$$\rho_a = 0.2766 + 0.02066(i/90) + 0.2953(i/90)^2 - 0.1416(i/90)^3 \tag{4}$$

where i is expressed in degrees.

Figure 1 shows the geometry of the problem in which all the distances are indicated in dimensionless quantities normalized by the mean earth radius. From the geometrical relationships depicted here, the view factors can be written as

$$F_e = \frac{1}{\pi}\int_V \frac{\cos\xi \cos\chi}{\imath^2}\, dS \qquad (V\text{: visible}) \tag{5a}$$

$$F_a = \frac{1}{\pi}\int_{V\&S} \frac{\cos\xi \cos\chi \cos\zeta}{\imath^2}\, dS \qquad (V\&S\text{: visible and sunlit}) \tag{5b}$$

where dS is an area element on the earth surface and $\imath$ the distance from a plate, apart r from the earth center, to dS. Equation (5a) is integrated over a spherical cap V which sees the plate. As clearly seen from Fig. 1, the integration range is limited by an angle defined as

$$\theta_m = \cos^{-1}(1/r) \tag{6}$$

Equation (5b) is then integrated over a sunlit portion $V\&S$ in the visible region V. From Fig. 1, the quantities associated with Eqs. (5a, 5b) are

$$dS = \sin\theta\, d\theta\, d\varphi \qquad (0 \leqq \theta \leqq \theta_m, \quad -\pi \leqq \varphi \leqq \pi) \tag{7}$$

$$\imath^2 = r^2 + 1 - 2r\cos\theta \tag{8}$$

$$\imath \cos\xi = r\cos\theta - 1 \tag{9}$$

$$\imath \cos\eta = r - \cos\theta \tag{10a}$$

$$\imath \sin\eta = \sin\theta \tag{10b}$$

$$\cos\chi = \cos\gamma \cos\eta + \sin\gamma \sin\eta \cos(\varphi - \phi) \tag{11}$$

$$\cos\zeta = \cos\psi_s \cos\theta + \sin\psi_s \sin\theta \cos\varphi \tag{12}$$

where θ and φ, respectively, are the colatitudinal angle and the azimuthal angle defining the position of dS, ξ the angle between $\imath$ and the normal to dS, η the angle between $-\imath$ and the counter radius vector E, χ the angle between $-\imath$ and the plate normal D, ζ the angle between the solar vector S and the normal to dS, ψ_s the angle between the radius vector $-$E and S, γ the angle between E and D, and ϕ the azimuthal

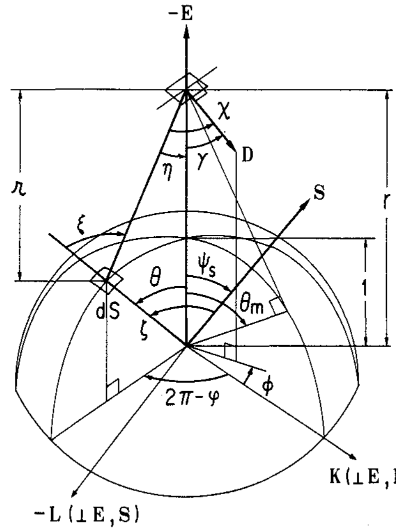

Fig. 1 Geometry of the problem.

angle showing the direction of D projected on the plane perpendicular to E.

For specifying ϕ, one introduces the vector L perpendicular to both E and S and defines the outer product of E and L as the vector K. The angles ψ_s, γ, and ϕ can now be calculated from the inner products SE, DE, DK, and DL. The results are

$$\cos\psi_s = -(s_x e_x + s_y e_y + s_z e_z) \equiv -w \tag{13}$$

$$\cos\gamma = d_x e_x + d_y e_y + d_z e_z \tag{14}$$

$$\sin\gamma \cos\phi = (d_x s_x + d_y s_y + d_z s_z - w\cos\gamma)/\sqrt{1-w^2} \tag{15a}$$

$$\sin\gamma \sin\phi = [(d_y s_z - d_z s_y)e_x + (d_z s_x - d_x s_z)e_y + (d_x s_y - d_y s_x)e_z]/\sqrt{1-w^2} \tag{15b}$$

where (s_x, s_y, s_z), (e_x, e_y, e_z), and (d_x, d_y, d_z) are the components of S, E, and D expressed in the inertia coordinates.

Earth-Oriented Panel

For an earth-oriented panel, the problem can remarkably be simplified because $\gamma = 0$, thereby, $\chi = \eta$. In this case, Eqs.(5a) and (5b) reduce to

$$\bar{F}_e = \frac{1}{\pi}\int_V \frac{\cos\xi \cos\eta}{\imath^2} dS = 1/r^2 \tag{16a}$$

$$\bar{F}_a = \frac{1}{\pi}\int_{V\&S} \frac{\cos\xi \cos\eta \cos\zeta}{\imath^2} dS \tag{16b}$$

As previously mentioned by Cunningham,[4,5] there are four possible relations defining the region $V\&S$: 1) if $0 \leqq \psi_s \leqq \pi/2 - \theta_m$, the region V is then fully sunlit; 2) if $\pi/2 - \theta_m < \psi_s < \pi/2$, two parts in it are then sunlit; 3) if $\pi/2 \leqq \psi_s < \pi/2 + \theta_m$, only one part in it is then sunlit; and 4) if $\pi/2 + \theta_m \leqq \psi_s$, it is then not illuminated by the sun. For cases 1–3 classified above, the areas of integration are: 1) $0 \leqq \theta \leqq \theta_m$ and $|\varphi| \leqq \pi$; 2) $|\varphi| \leqq \pi$ when $0 \leqq \theta \leqq \pi/2 - \psi_s$ while $|\varphi| \leqq \varphi_m$ when $\pi/2 - \psi_s \leqq \theta \leqq \theta_m$; and 3) $\psi_s - \pi/2 \leqq \theta \leqq \theta_m$ and $|\varphi| \leqq \varphi_m$, where $\varphi_m = \cos^{-1}(-\cot\psi_s \cot\theta)$, derived from Eq. (12) with $\zeta = \pi/2$.

Upon integration, Eq. (16b) becomes

$$\bar{F}_a = \frac{\cos\psi_s}{8r^3}\left[2(r^3 + r + 2) - (r^2-1)^2 \ln\left|\frac{r+1}{r-1}\right|\right] \quad \text{if} \quad 0 \leqq \psi_s \leqq \pi/2 - \theta_m \tag{17a}$$

$$= \frac{\cos\psi_s}{8r^3}\left[2r^2 \frac{r^2+1+2r\sin\psi_s}{r^2+1-2r\sin\psi_s}\cos^2\psi_s + 2r(r^2+1)(1-\sin\psi_s) - (r^2-1)^2 \ln\left|\frac{r^2+1-2r\sin\psi_s}{(r-1)^2}\right|\right] + B + C \quad \text{if} \quad \pi/2 - \theta_m < \psi_s < \pi/2 \tag{17b}$$

$$= B + C \quad \text{if} \quad \pi/2 \leqq \psi_s < \pi/2 + \theta_m \tag{17c}$$

$$= 0 \quad \text{if} \quad \pi/2 + \theta_m \leqq \psi_s \leqq \pi \tag{17d}$$

The constants B and C in Eqs. (17b) and (17c) are expressed in

$$B = \frac{2}{\pi}\cos\psi_s \int_{1/r}^{\sin\psi_s} \frac{(rt-1)(r-t)t}{(r^2+1-2rt)^2}\cos^{-1}\left(-\frac{t\cot\psi_s}{\sqrt{1-t^2}}\right) dt \tag{18a}$$

$$C = \frac{2}{\pi}\int_{1/r}^{\sin\psi_s} \frac{(rt-1)(r-t)}{(r^2+1-2rt)^2}\sqrt{\sin^2\psi_s - t^2}\, dt \tag{18b}$$

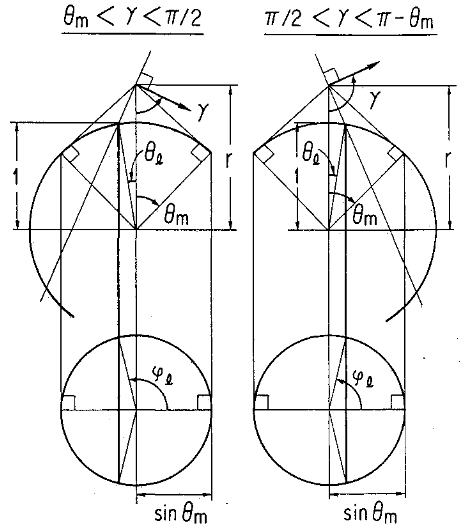

Fig. 2 Visible terrestrial portion.

Arbitrarily Oriented Panel

For an arbitrarily oriented panel, the integral calculus in Eq. (5a) becomes rather complicated but will be written as

$$F_e = \bar{F}_e f_\gamma \tag{19}$$

A problem set up here is to find an expression of the factor f_γ which depends on both γ and θ_m. As treated before by Cunningham,[6] the problem is divided into three parts. The first part arises when the panel is so oriented that the earth appears as a circular disk. The second part occurs when it is so oriented that the earth looks like a chipped disk. This case of interest is illustrated with Fig. 2. The third part corresponds to an occasion where the earth disappears from sight. These three are therefore, specified as 1) $0 \leqq \gamma \leqq \theta_m$; 2) $\theta_m < \gamma < \pi - \theta_m$; and 3) $\pi - \theta_m \leqq \gamma \leqq \pi$. If $0 \leqq \gamma \leqq \theta_m$, Eq. (5a) is then integrable and results in $F_e = \cos\gamma/r^2 = \bar{F}_e \cos\gamma$. It is also clear that $F_e = 0$ if $\pi - \theta_m \leqq \gamma \leqq \pi$.

In such a configuration as shown in Fig. 2, it is quite difficult to integrate Eq. (5a) but it should be noticed that F_e is nearly proportional to the sunlit to total disk area ratio η_ℓ. From Fig. 2, one easily obtains

$$\eta_\ell = (\varphi_\ell - \sin\varphi_\ell \cos\varphi_\ell)/\pi \tag{20}$$

The angle φ_ℓ is derived from a relation, $\sin\theta_\ell = \mp \sin\theta_m \cos\varphi_\ell$, to give:

$$\varphi_\ell = \cos^{-1}(-\sin\theta_\ell/\sin\theta_m) \quad \text{if} \quad \theta_m < \gamma < \pi/2 \tag{21a}$$

$$= \pi/2 \quad \text{if} \quad \gamma = \pi/2 \tag{21b}$$

$$= \cos^{-1}(\sin\theta_\ell/\sin\theta_m) \quad \text{if} \quad \pi/2 < \gamma < \pi - \theta_m \tag{21c}$$

where $\sin\theta_m = \sqrt{r^2 - 1}/r$. Then, the angle θ_ℓ is derived from another relation, $r\cos\gamma = \cos(\gamma \mp \theta_\ell)$. This equation yields a solution of the form:

$$t = (\sin\gamma - \sqrt{1 - r^2\cos^2\gamma})/(r + 1)|\cos\gamma| \tag{22}$$

where the relation between θ_ℓ and t is

$$\sin\theta_\ell = 2t/(1 + t^2) \tag{23}$$

Judging from a fact that $\cos\gamma = 1/r$ and $\eta_\ell = 1$ when $\gamma = \theta_m$, the factor f_γ will naturally be proportional to $1/r$ in the region $\theta_m < \gamma < \pi - \theta_m$ because of continuity. Finally, the result becomes

$$f_\gamma = \cos\gamma \quad \text{if} \quad 0 \leqq \gamma \leqq \theta_m \tag{24a}$$

$$\simeq \eta_\ell/r \quad \text{if} \quad \theta_m < \gamma < \pi - \theta_m \tag{24b}$$

$$= 0 \quad \text{if} \quad \pi - \theta_m \leqq \gamma \leqq \pi \tag{24c}$$

Then, as seen from Fig. 2, another condition that $\phi' - \varphi_\ell \leqq \varphi \leqq \phi' + \varphi_\ell$ holds for a visible region of the circular disk.

All possible combinations of these two conditions are the following five: 1) $\varphi_k \leqq \varphi_\ell$ and $0 \leqq \phi' \leqq \varphi_\ell - \varphi_k$, 2) $\varphi_k \geqq \varphi_\ell$ and $0 \leqq \phi' \leqq \varphi_k - \varphi_\ell$, 3) $\varphi_k \leqq \varphi_\ell$ and $\varphi_\ell - \varphi_k \leqq \phi' \leqq \varphi_k + \varphi_\ell$, 4) $\varphi_k \geqq \varphi_\ell$ and $\varphi_k - \varphi_\ell \leqq \phi' \leqq \varphi_k + \varphi_\ell$, and 5) $\varphi_k + \varphi_\ell \leqq \phi' \leqq \pi$. After transposition, they turn into: 1) $\phi' - \varphi_\ell \leqq -\varphi_k$ and $\phi' + \varphi_\ell \geqq \varphi_k$; 2) $\phi' - \varphi_\ell \geqq -\varphi_k$ and $\phi' + \varphi_\ell \leqq \varphi_k$; 3) $\phi' - \varphi_\ell \geqq -\varphi_k$ and $\phi' + \varphi_\ell \geqq \varphi_k$; 4) $\phi' - \varphi_\ell \geqq -\varphi_k$ and $\phi' + \varphi_\ell \geqq \varphi_k$; and 5) $\phi' - \varphi_\ell \geqq \varphi_k$. Figure 3 is placed here for better understanding of angular relations. It can be shown from Fig. 3 that all the sunlit portion comes visible or invisible as the case may be first or fifth, and also that there exist invisible sunlit regions under other circumstances. The factor f_ϕ should, therefore, be defined as a rate at which the projected sunlit portion is visible; that is, as an area ratio of a sector hatched in Fig. 3 to the sector $2\varphi_k$. Thus, one has

$$f_\phi = 1 \quad \text{if} \quad \varphi_k \leqq \varphi_\ell \quad \text{and} \quad 0 \leqq \phi' \leqq \varphi_\ell - \varphi_k \tag{28a}$$

$$= \varphi_\ell/\varphi_k \quad \text{if} \quad \varphi_k \geqq \varphi_\ell \quad \text{and} \quad 0 \leqq \phi' \leqq \varphi_k - \varphi_\ell \tag{28b}$$

$$= (\varphi_k + \varphi_\ell - \phi')/2\varphi_k \quad \text{if} \quad |\varphi_k - \varphi_\ell| \leqq \phi' \leqq \varphi_k + \varphi_\ell \tag{28c}$$

$$= 0 \quad \text{if} \quad \varphi_k + \varphi_\ell \leqq \phi' \leqq \pi \tag{28d}$$

With regards Eq. (5b), there are three possibilities defining F_a for an arbitrarily oriented panel as well as an earth-oriented one. They principally depend on angular relations between ψ_s and θ_m and are also classified as 1) $0 \leqq \psi_s \leqq \pi/2 - \theta_m$; 2) $\pi/2 - \theta_m < \psi_s < \pi/2 + \theta_m$; and 3) $\pi/2 + \theta_m \leqq \psi_s \leqq \pi$. As easily understood from the geometry, if $0 \leqq \psi_s \leqq \pi/2 - \theta_m$, all the terrestrial portion seen from the plate are then fully sunlit under any azimuthal direction specified by ϕ. Then, under the condition that $\pi/2 - \theta_m < \psi_s < \pi/2 + \theta_m$, the possibly visible terrestrial region forming a chipped disk will fully or partly be sunlit, or may not be illuminated by the sun. The factor F_a here depends not only on γ but also on ϕ. In the case where $\pi/2 + \theta_m \leqq \psi_s \leqq \pi$, there is no albedo radiation incident upon the plate because all the sunlit hemisphere is invisible. Since the angular dependence of F_a on γ will again be evaluated by f_γ, the factor F_a can eventually be written as

$$F_a = \bar{F}_a f_\gamma \quad \text{if} \quad 0 \leqq \psi_s \leqq \pi/2 - \theta_m \tag{25a}$$

$$F_a \simeq \bar{F}_a f_\gamma f_\phi \quad \text{if} \quad \pi/2 - \theta_m < \psi_s < \pi/2 + \theta_m \tag{25b}$$

$$F_a = 0 \quad \text{if} \quad \pi/2 + \theta_m \leqq \psi_s \leqq \pi \tag{25c}$$

where $\bar{F}_a$ and f_γ are, respectively, given by Eqs. (17) and (24), and f_ϕ is a factor showing contributions of ϕ to F_a.

The problem now arrives at determining f_ϕ. Its practical expression can be obtained with the help of projection geometry. On the KL plane shown in Fig. 1, the sunlit portion lies in a fan-shaped area satisfying a condition that $-\varphi_k \leqq \varphi \leqq \varphi_k$, where φ_k is expressed as

$$\varphi_k = \cos^{-1}(-\cot\psi_s \cot\theta_m) \tag{26}$$

Equation (26) is derived from Eq. (12) with $\theta = \theta_m$ and $\zeta = \pi/2$. Taking advantage of symmetry of this area with respect to the reference direction as $\varphi = 0$, one replaces ϕ with

$$\phi' = \phi \quad \text{if} \quad 0 \leqq \phi \leqq \pi \tag{27a}$$

$$= 2\pi - \phi \quad \text{if} \quad \pi < \phi < 2\pi \tag{27b}$$

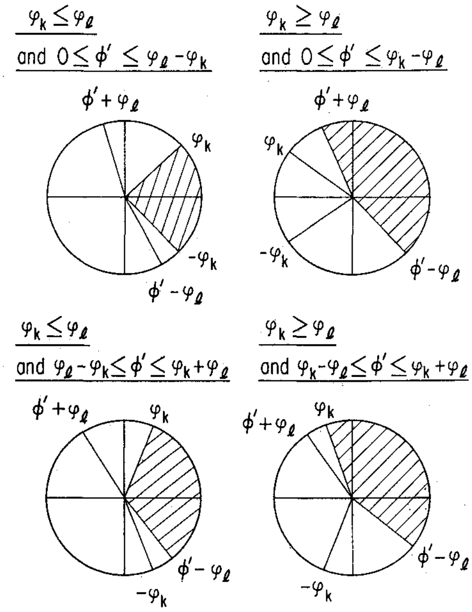

Fig. 3 Visible part of projected sunlit region.

References

[1]Katz, A. J., "Determination of Thermal Radiation Incident upon the Surfaces of an Earth Satellite in an Elliptical Orbit," IAS Paper 60-58, Los Angeles, CA, June/July 1960.

[2]Hrycak, P., "Effects of Secondary Radiation on an Orbiting Satellite," *ARS Journal*, Vol. 32, No. 8, 1962, pp. 1294–1295.

[3]Ballinger, J. C., Elizalde, J. C., and Christensen, E. H., "Thermal Environment of Interplanetary Space," Presented at the Society of Automotive Engineers National Aeronautic Meeting, Paper No. 344B, New York, NY, 1961.

[4]Cunningham, F. G., "Earth Reflected Solar Radiation Input to Spherical Satellites," NASA TN D-1099, Oct. 1961.

[5]Cunningham, F. G., "Earth-Reflected Solar Radiation Incident upon Spherical Satellites in General Elliptical Orbits," NASA TN D-1472, Feb. 1963.

[6]Cunningham, F. G., "Power Input to a Small Flat Plate from a Diffusely Radiating Sphere with Application to Earth Satellites," NASA TN D-710, Aug. 1961.

[7]Cunningham, F. G., "Power Input to a Small Flat Plate from a Diffusely Radiating Sphere with Application to Earth Satellites: the Spinning Plate," NASA TN D-1545, Feb. 1963.

[8]Cunningham, F. G., "Earth-Reflected Solar Radiation Incident upon an Arbitrarily Oriented Spinning Flat Plate," NASA TN D-1842, July 1963.

[9]Powers, E. I., "Thermal Radiation to a Flat Surface Rotating about an Arbitrary Axis in an Elliptical Earth Orbit: Application to Spin-Stabilized Satellites," NASA TN D-2147, April 1964.

[10]Bannister, T. C., "Radiation Geometry Factor between the Earth and a Satellite," NASA TN D-2750, July 1965.

[11]Watts, R. G., "Radiant Heat Transfer to Earth Satellites," Transactions of the ASME, *Journal of Heat Transfer*, Vol. 87, Aug. 1965, pp. 369–373.

[12]Skladany, J. T., and Rochkind, A. B., "Determination of Net Thermal Energy Incident on a Satellite," ASME Paper 67-HT-56, Seattle, WA, Aug. 1967.

[13]Doenecke, J., "Thermal Radiations Absorbed by a Partially Obscured Spacecraft," *Astronautica Acta*, Vol. 15, Dec. 1969, pp. 107–117.

[14]Finch, H. L., Sommerville, D., Vogt, R., and Bland, D., "A Computer Program for Calculating External Thermal Radiation Heat Loads and Temperatures of Spacecraft Orbiting the Planets or the Moon," NASA TR R-278, Dec. 1968.

[15]Turner, R. C., "NEVADA Software Package User's Manual," 7th ed., Turner Associates, Brea, CA, Jan. 1980.

[16]Jensen, C. L., and Goble, R. G., "TRASYS II User's Manual," Martin Marietta, MCR-73-105 (NAS9-15832), ReV. 5, Denver, CO, June 1983.

[17]Prenger, Jr., F. C., and Patterson, W. C., "Earth Albedo as Determined from Skylab Data," *Journal of Spacecraft and Rockets*, Vol. 13, April 1976, pp. 244–247.

Laminar Forced Convection in Circular Duct Inserted with a Longitudinal Rectangular Plate

Jun-Dar Chen* and Shou-Shing Hsieh†
National Sun Yat-Sen University, Kaohsiung, Taiwan, Republic of China

I. Introduction

LAMINAR forced convection in circular duct with a longitudinal arbitrary-shaped inner core is encountered in a wide variety of engineering situations, such as a double-pipe heat exchanger, gas-cooled electrical cables, and a tube with removable insert as a heat transfer augmentative device in a tubular recuperator. Excellent surveys of laminar forced convections in circular and noncircular annular ducts have been presented by Shah and London[1] and Shah and Bhatti.[2] It was found from these surveys that, while the laminar forced convection in circular annulus had been thoroughly studied, it was apparent that very little was known about that in noncircular annulus. The regular polygon had been extensively considered as the shape of the inner core in studies of noncircular annulus.[1,2] As one of the tubeside augmentative devices, the rectangularly shaped inner core is frequently used in practical tubular recuperators. However, it has received very little attention except with the unity aspect ratio, i.e., square shape.

Received Aug. 31, 1990; revision received Dec. 10, 1990; accepted for publication Dec. 17, 1990.

*Graduate Student, Department of Mechanical Engineering.

†Professor and Chairman, Department of Mechanical Engineering. Member AIAA.

The point-matching method and the least squares approximation method has been applied to analyze the laminar forced convection in a circular duct with a concentric square core under the thermal boundary conditions of axially uniform heat flux and peripherally uniform temperature on the walls.[1,2] Recently, Solanki et al.[3–6] studied similar problems in which thermal boundary conditions of axially and peripherally uniform heat flux at the inner wall and insulated outer wall with peripherally constant temperature were used. The Galerkin finite element method was adopted in their numerical studies, which provided the flow[3] and temperature[4] patterns inside the noncircular annulus. However, only the flowfield was investigated in their experimental works.[5,6] By a square core of radius ratio 0.6783, an experimental assessment for numerical result of the *fRe* factor was made.[6] Excellent agreement substantiated the reliability of the numerical results. Despite the foregoing discussion, it seems that no results of a circular duct with an eccentric noncircular inner core are available in the open literature.

This paper presents a numerical study for thermally developed laminar forced convection in a heated circular duct inserted concentrically or vertically eccentrically with a longitudinal rectangular adiabatic plate. The flow passage is schematically depicted in Fig. 1 where relative geometric quantities are also shown. In addition to the flow and temperature patterns, effects of aspect ratio of insert (L/H), radius ratio of the circumscribed circle of insert to duct (RR), and vertically eccentric installation of the insert, on the laminar forced convection are determined.

II. Theoretical Analysis

Consider steady, laminar fully developed flow with constant fluid properties in the noncircular annulus of Fig. 1 in which the duct is assumed to be of axially uniform heat flux, q''_{in}, with peripherally constant wall temperature. The mathematical formulation and solution procedure are outlined in great detail by Chen and Hsieh[7] and only a brief description is presented here. The constant axial temperature rising rate is related to q''_{in} via overall heat balance. The radius of duct, R_o, $(-\mathrm{d}p/\mathrm{d}z)R_o^2/\mu$ and $q''_{in}R_o/k$ are used to scale length, velocity, and relative temperature (with respect to the constant as $EV = (e_v/R_o)/(1 - RR)$). Here $\mathrm{d}p/\mathrm{d}z$ = axial pressure gradient, μ = fluid dynamic viscosity, k = fluid thermal conductivity, and e_v = vertical eccentricity. Under the above assumptions, the dimensionless axial momentum and energy conservation equations are formulated as

$$\frac{\partial^2 W}{\partial X^2} + \frac{\partial^2 W}{\partial Y^2} + 1 = 0 \tag{1}$$

$$\frac{\partial^2 T}{\partial X_2} + \frac{\partial^2 T}{\partial Y^2} - \frac{WP_o}{M_m A_f} = 0 \tag{2}$$

where P_o and A_f are dimensionless outer wall perimeter and flow area and W_m is dimensionless mean velocity of the pas-

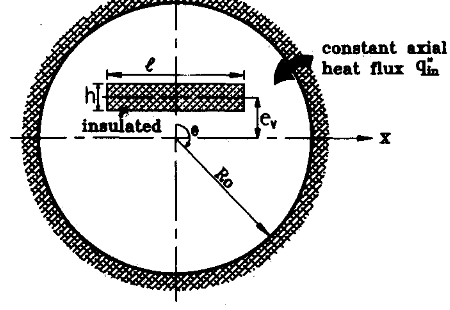

Fig. 1 Noncircular annular duct.